Ultrasonics Sonochemistry 105 (2024) 106853

Contents lists available at ScienceDirect

Ultrasonics Sonochemistry

journal homepage: www.elsevier.com/locate/ultson

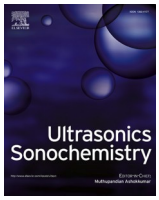

Enhanced cavitation dose and reactive oxygen species production in microbubble-mediated sonodynamic therapy for inhibition of Escherichia coli and biofilm

Changlong Li [a,1], Fengmeng Teng [b,1], Fengmin Wu [a,*], Hui Zhang [a], Chunbing Zhang [b,*], Dong Zhang [a,c,*]

[a] Department of Applied Physics, School of Science, Harbin University of Science and Technology, Harbin 150080, China
[b] Affiliated Hospital of Nanjing University of Chinese Medicine, Nanjing 210023, China
[c] Key Laboratory of Modern Acoustics (MOE), Department of Physics, Collaborative Innovation Center of Advanced Microstructure, Nanjing University, Nanjing 210093, China

ARTICLE INFO

Keywords:
Sonodynamic therapy
Cavitation
Microbubble
Biofilm

ABSTRACT

Sonodynamic therapy (SDT) is an emerging antibacterial therapy. This work selected hematoporphyrin monomethyl ether (HMME) as the sonosensitizer, and studied the enhanced inhibition effect of Escherichia coli and biofilm by microbubble-mediated cavitation in SDT. Firstly, the influence of microbubble-mediated cavitation effect on different concentrations of HMME (10 μg/ml, 30 μg/ml, 50 μg/ml) was studied. Using 1,3-diphenylisobenzofuran (DPBF) as an indicator, the effect of microbubble-mediated cavitation on the production of reactive oxygen species (ROS) was studied by absorption spectroscopy. Secondly, using agar medium, laser confocal microscopy and scanning electron microscopy, the effect of microbubble-mediated cavitation on the activity and morphology of bacteria was studied. Finally, the inhibitory effect of cavitation combined with SDT on biofilm was evaluated by laser confocal microscopy. The research results indicate that: (1) Microbubble-mediated ultrasound cavitation can significantly increase cavitation intensity and production of ROS. (2) Microbubble-mediated acoustic cavitation can alter the morphological structure of bacteria. (3) It can significantly enhance the inhibition of SDT on the activity of Escherichia coli and its biofilm. Compared with the control group, the addition of microbubbles resulted in an increase in the number of dead bacteria by 61.7 %, 71.6 %, and 76.2 %, respectively. The fluorescence intensity of the biofilm decreased by 27.1 %, 80.3 %, and 98.2 %, respectively. On the basis of adding microbubbles to ensure antibacterial and biofilm inhibition effects, this work studied the influence of cavitation effect in SDT on bacterial structure, providing a foundation for further revealing the intrinsic mechanism of SDT.

1. Introduction

Pathogenic microorganisms are an ever-growing concern for public health. Though the advent of antibiotics has somewhat alleviated this problem, the use of antibiotics and other antimicrobial drugs may lead to antibiotic resistance due to mutations, and weaken the effectiveness of antimicrobial drugs [1–5]. It is estimated that if the development of bacterial resistance cannot be curbed, by 2050, the number of deaths caused by bacterial resistance could rapidly increase to 10 million per year, far exceeding the number of deaths from cancer [6–7]. In addition, biofilm formation further enhances bacterial resistance after bacteria attach and multiply extensively. Bacterial biofilm is composed of microbial communities, and its protective matrix structure leads to a hindering antibiotic effectiveness up to 1000-fold compared to free-floating bacteria and facilitating development of antibiotic resistance [8]. The main component of biofilm is extracellular polymeric substances (EPS), whose main role is to protect bacterial cell in the biofilm from dehydration in adverse environment, and to defend immune substances

* Corresponding authors at: Department of Applied Physics, School of Science, Harbin University of Science and Technology, Harbin, 150080, China (F. Wu); Affiliated Hospital of Nanjing University of Chinese Medicine, Nanjing 210023, China (C. Zhang); Key Laboratory of Modern Acoustics (MOE), Department of Physics, Collaborative Innovation Center of Advanced Microstructure, Nanjing University, Nanjing, 210093, China (D. Zhang).
E-mail addresses: fmwu@hrbust.edu.cn (F. Wu), zzzzcb99_nj@163.com (C. Zhang), dzhang@nju.edu.cn (D. Zhang).
[1] These authors contributed equally to this work.

https://doi.org/10.1016/j.ultsonch.2024.106853
Received 1 January 2024; Received in revised form 9 March 2024; Accepted 22 March 2024

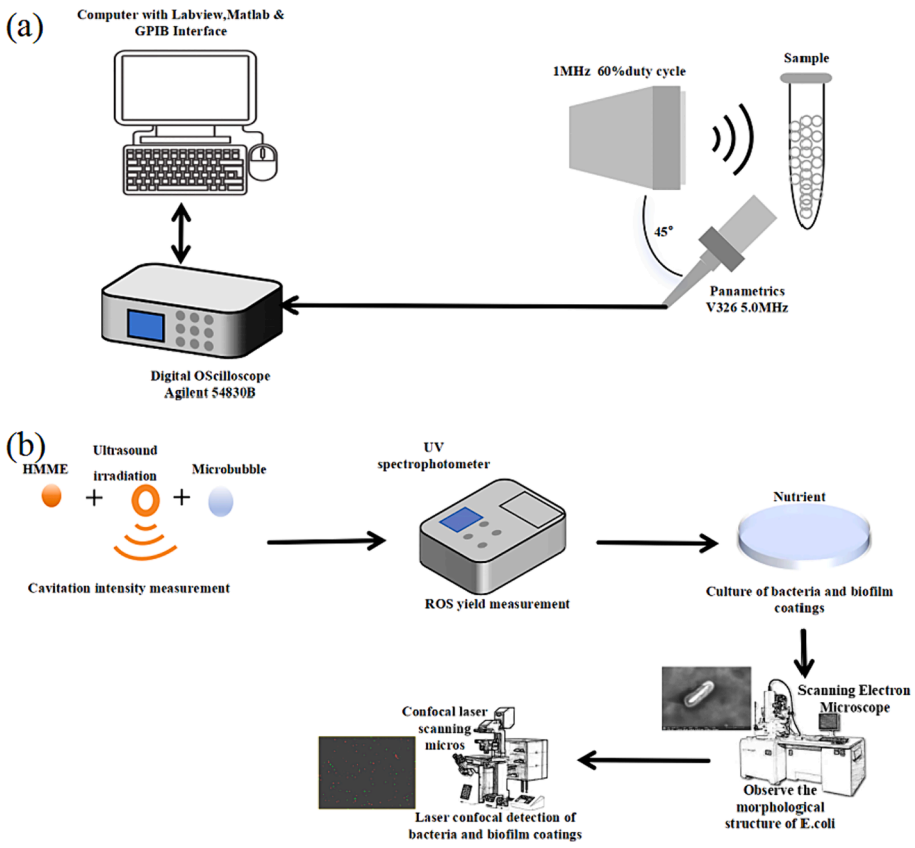

Fig. 1. (a) The schematic diagram of the experimental apparatus. Experimental flow chart. (b) The experimental process of this study including cavitation intensity detection, active oxygen production detection, antibacterial experiment of agar medium, observation of Escherichia coli by laser confocal microscope, observation of the morphology and structure of Escherichia coli by scanning electron microscope, and observation of Escherichia coli biofilm by laser confocal microscope.

produced by the body and exogenous antimicrobial drugs [9–11]. Faced with increasing bacterial resistance and the threat of bacterial biofilms to human health, there is an urgent need for a method that can kill bacteria and inhibit biofilm without enhancing bacterial resistance.

Recently, photodynamic therapy has been used to the treatment of bacterial infections, which can effectively avoid bacterial resistance. The application scope of photodynamic therapy has expanded from the initial tumor treatment to the inhibition of bacteria biofilms, fungi and other microorganisms [12–21]. Photosensitizers accumulate in tumor lesion areas, laser excitation is used to activate photosensitizers, producing reactive oxygen species (ROS), thereby killing tumor cells. However, photodynamic therapy also has obvious disadvantages, i.e. the depth of laser action is limited. Consequently, an alternative method named sonodynamic therapy (SDT) has attracted much attention [22–27]. Researchers have found that both the sole use of ultrasound and its combination with other antimicrobial methods exhibit excellent inhibitory effects on various microorganisms, such as bacteria, fungi, and viruses[26–32]. Utilizing microbubble technology as a key approach to optimizing SDT for enhanced treatment effects has attracted widespread attention [33–35]. When ultrasound is irradiated onto a sonosensitizer, it can cause the sonosensitizer to be in an excited state and produce ROS [36]. Due to its strong penetration ability, non-invasiveness, lack of resistance, and activity only when irradiated by ultrasound, SDT has become a widely concerned emerging antimicrobial treatment. Currently, the mechanism of SDT has not been fully explained. The existing explanations can be mainly divided into three categories: (1) The shear force caused by the movement of cavitation bubbles on the surface of biological membranes due to the cavitation effect of ultrasound. With the aid of shear force, sonosensitizers can enter cells, causing cell damage and destruction [37]. (2) Strong light activated by the collapse of cavitation bubbles activates sonosensitizers [38]. (3) Ultrasonic cavitation activates the sonosensitizers, leading to the production of ROS, which can undergo oxidation reactions with cell components such as proteins, membrane lipids, and DNA, damaging cell structure and killing cells [39]. Considering the cavitation effect brought by ultrasound, this paper aims to enhance the inhibition of bacteria and their biofilms using SDT combined with microbubble-mediated cavitation effects, and investigates the underlying mechanism. Hematoporphyrin monomethyl ether (HMME) was selected as the sonosensitizer for SDT, and Sonovue microbubbles (MBs) were used in conjunction with HMME. In the experiment, the cavitation intensity was detected by passive cavitation detection (PCD), the antibacterial effect was detected by laser confocal microscopy and agar culture medium, the morphology structure of Escherichia coli was observed by scanning electron microscope (SEM), and the growth change of bacterial biofilm was observed by laser confocal microscopy.

2. Materials and methods

2.1. Cultivation of strains

Using Escherichia coli standard strain (ATCC25922) as the experimental object for antimicrobial experiments. First, the Escherichia coli standard strain was inoculated into a liquid culture medium and cultured for 24 h at 37 °C and 5 % carbon dioxide in a culture box (Thermo scientific, forma370) to increase the bacterial population. Then, bacteria were picked up with a loop and inoculated on an agar plate, which was then cultured for 24 h at 37 °C and 5 % carbon dioxide in a culture box for future use. Each time during the experiment, a single colony was picked from the agar plate, dissolved in normal saline, and adjusted for bacterial concentration for future use.

2.2. Ultrasonic exposure and passive cavitation detection (PCD) systems

Fig. 1(a) shows the schematic diagram of the experimental apparatus. A waveform generator (33250A; Agilent, Santa Clara, CA, USA) produced a 1 MHz sine pulse with a fixed duty cycle of 60 %, a pulse-repetition frequency (PRF) of 100 Hz, and 6000 cycles per burst. The signal was amplified through a radio frequency power amplifier (ATA-4315; Xi'an Antai, Shaanxi, Xi'an, China), and used to excite a 1 MHz plane transducer (diameter 3 cm, effective area 2 cm^2). The radiation force balance (RFB-2000, ONDA, USA) was used to calibrate the ultrasonic intensity used in the experiment, with a measurement distance of 2 mm and an effective area of 2 cm^2 during the calibration process. The calibrated ultrasonic intensities (spatial-average time-averaged, I_{SATA}) were 0.15w/cm^2, 0.25w/cm^2, 0.35w/cm^2, 0.45w/cm^2, 0.55w/cm^2, 0.65w/cm^2, 0.75w/cm^2, 0.85w/cm^2, 0.95w/cm^2, 1.05w/cm^2, 1.25w/cm^2, 1.50w/cm^2, 1.75w/cm^2. Placed the HMME solutions at various concentrations prepared with physiological saline into a 80 ml culture bottle, aligned the culture bottle with the transducer axially, fixed it at a position 1 mm away from the surface of the transducer, and then used ultrasound to act on the solution in the culture bottle. The treatment time of each ultrasonic intensity on the sample is 5 s, and the main component of the microbubbles used is sulfur hexafluoride. All experiments were carried out in a water tank filled with degassed water. During the experiments, the calibrated sound intensity mentioned above was used to act on the samples. The 5 MHz transducer (Panasonic V326, USA) was adopted, with an angle of 45° between the hydrophone and the ultrasonic source, for collecting bubble scattering and emission signals based on PCD measurements. The measured PCD signals were finally digitized by an oscilloscope (54830B, Agilent, Santa Clara, CA, USA). Based on extensive research on cavitation dosage [40–42], the detailed information about the detection of inertial cavitation dose (ICD) in this work was presented in the supplementary materials.

2.3. Experimental protocols

2.3.1. Detection of reactive oxygen production

Experimental grouping was as follows: the concentration of HMME was set at 10ug/ml, 30ug/ml and 50ug/ml. The cavitation intensity was measured for each concentration of HMME with/without MBs (the ratio of MBs to sonosensitizer is 1:400). Used 1,3-diphenyl benzofuran (DPBF, Aladdin Reagent Co., Ltd.) with a concentration of 0.17 mg/ml as an indicator and mixed it with each concentration of sonosensitizer separately. Stored them in a 4 ml culture dish and applied ultrasound to the solution for 0 min, 1 min, 3 min, and 5 min respectively. The change in absorbance of DPBF was measured by a UV spectrophotometer (Shanghai Lengguang Technology Co., Ltd, 1901PC) to indicate the amount of ROS generated.

2.3.2. Antibacterial experiment on agar culture medium

In the antibacterial experiment, standard strains of Escherichia coli were selected and cultured on agar plates for 24 h. The colonies were picked and dissolved in physiological saline using a sterile inoculation ring. Then, the turbidity of the bacteria was measured using a Densi CHEK turbidimeter, and the turbidity of Escherichia coli was adjusted to 1.0 McDonnell's unit.

In the experiment, the method of inoculating with agar medium was used to observe the trend of bacterial activity changes. The control group consisted of 200ul of Escherichia coli added to 4 ml of physiological saline, without ultrasound irradiation or the addition of sonosensitizer. A 10ul inoculum was used to pick out the bacteria and inoculate them into a nutrient agar medium (Antu Biotechnology Co., Ltd., 20230812B, stored at 2℃-8℃). The medium was incubated for 12 h at 37℃ in a 5 % carbon dioxide constant temperature incubator (Thermo cosmetic, forma370). Four experimental groups were used, i.e. the ultrasound group, the sonosensitizer group without ultrasound irradiation, the SDT group, and the SDT with MBs group. 200ul of Escherichia coli with a turbidity of 1.0 was added to 4 ml of physiological saline. The ultrasound group was treated with ultrasound (1 MHz, 1.5w/cm^2, 60 % duty cycle) for 30 min; the sonosensitizer group was added with a concentration of 50ug/ml of HMME but without ultrasound irradiation; the SDT group was added with a concentration of 50ug/ml of HMME, and subjected to ultrasound (1 MHz, 1.5w/cm^2, 60 % duty cycle) for 30 min; the SDT with MBs group was added with a concentrations of 10ug/ml, 30ug/ml, and 50ug/ml of HMME and MBs (the ratio of MBs to sound sensitizer is 1:400), and subjected to ultrasound (1 MHz, 1.5w/cm^2, 60 % duty cycle) for 30 min. During the ultrasonic process, a circulating degassed water was used as a coupling agent between the ultrasonic probe and the culture dish to avoid thermal effects during the experiment. Furthermore, a thermocouple was employed to monitor temperature changes throughout the experiment. The monitoring results indicated that the solution temperature did not increase by more than 1℃ during the experiment. After experimental treatment, took a 10ul inoculum and inoculate the bacteria into a nutrient agar medium (Antu Biotechnology Co., Ltd., 20230812B, stored at 2 ℃-8 ℃), and incubated in a constant temperature incubator at 37 ℃ and 5 % carbon dioxide for 12 h.

2.3.3. Inhibition of Escherichia coli based on laser confocal microscopy

Two experimental groups were used, i.e. the SDT group and the SDT with MBs group. Here, HMME with concentrations of 10ug/ml, 30ug/ml, and 50ug/ml, as well as MBs (the ratio of MBs quantity to sonosensitizer quantity is 1:400) were added. 200ul of Escherichia coli was added into 4 ml of each concentration of sonosensitizer solution. After ultrasonic treatment (1 MHz, 1.5w/cm^2, 60 % duty cycle) for 30 min, the treated bacteria were centrifuged at 3500r/min for 5 min. The supernatant was discarded, and 1 ml of phosphate buffer solution (PBS) was added to mix and wash twice. The death and survival of Escherichia coli were observed using a laser confocal microscope (Olympus, FV3000). The dead and living bacteria were stained using a SYTO/PI double staining kit (Shanghai Maokang Biotechnology Co., Ltd., stored at −20 °C). After mixing 1.5ul of SYTO and PI reagents, they were mixed and stained in the dark for 15 min. Then, the laser confocal microscope (Olympus, FV3000) was used for observation. Live bacteria appear green, while dead bacteria appear red. The Escherichia coli inhibition experiment with MBs was conducted using the same experimental method as above. Image J software was used to statistically analyze the change in the proportion of dead bacteria to live bacteria. The average value and standard deviation of the statistical results were calculated to obtain the number of dead or living bacteria in the image. The number of bacteria in different sonosensitizer concentrations and with or without MBs was statistically analyzed using the above method.

2.3.4. Morphological and structural changes of Escherichia coli based on scanning electron microscopy

After the SDT with MBs on bacteria, centrifuged at a speed of 3000r-4000r, removed the supernatant, added 1 ml PBS with a pH of 7.2–7.4 to clean three times. After centrifugation, used 2.5 % glutaraldehyde to fix the morphology structure of Escherichia coli for 12 h, fixed the morphology structure of Escherichia coli by centrifuging PBS three times. During dehydration, dehydrated the sample with ethanol water solution at concentrations of 30 %, 50 %, 70 %, 80 %, and 90 %, each dehydration step took about 15 min, dehydrated and then centrifuged, then dehydrated in 100 % ethanol for 15 min twice, after dehydration, centrifuged, placed the sample in a mixed solution of ethanol and *tert*-butanol at a ratio of 1:1 for 15 min, then centrifuged. Then replaced the alcohol with pure *tert*-butanol twice, each time for 15 min, finally froze dry for 24 h using a freeze dryer, after treatment, observed the morphology structure of bacteria using a scanning electron microscope (Helios 600i).

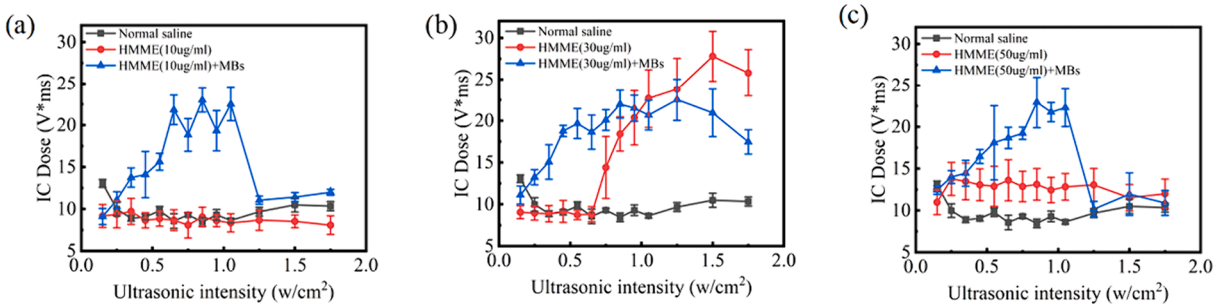

Fig. 2. Inertial cavitation dose (ICD) versus ultrasonic intensity of HMME at different concentrations. (a) 10ug/ml, (b) 30ug/ml and (c) 50ug/ml respectively.

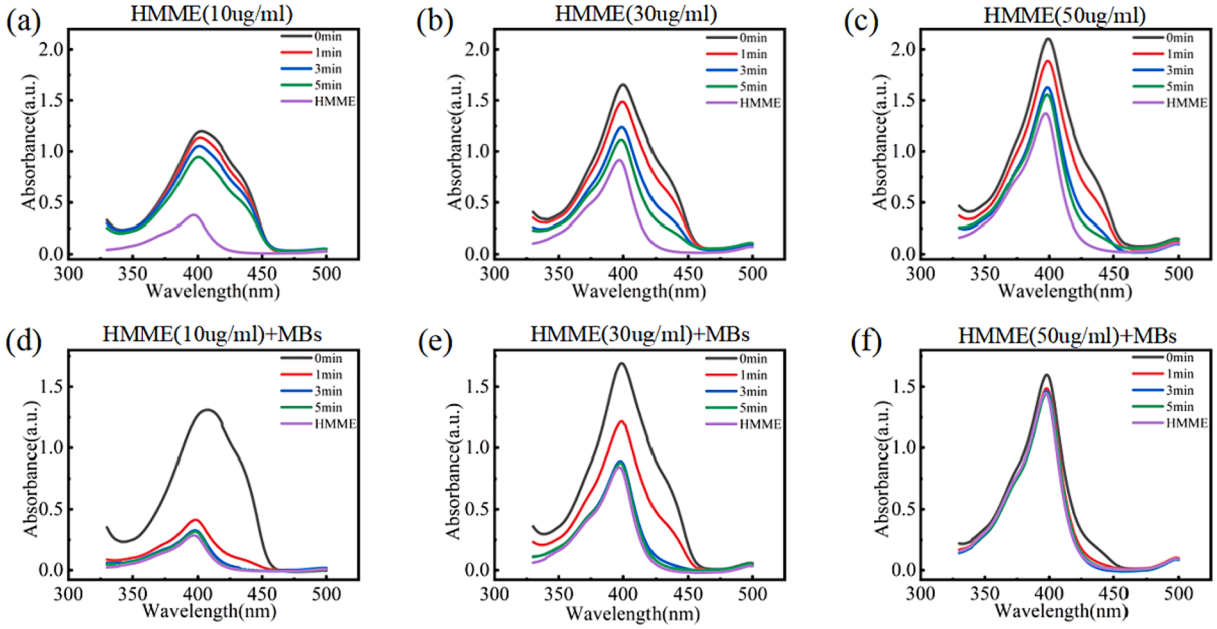

Fig. 3. The production of ROS was detected by measuring the change in UV absorbance of DPBF. (a), (b), and (c) are the curves showing the change in absorbance over time when HMME at concentrations of 10ug/ml, 30ug/ml, and 50ug/ml respectively; (d), (e), and (f) are the curves showing the change in DPBF over time when MBs were added under the same HMME concentrations.

2.3.5. Inhibition of Escherichia coli biofilm based on laser confocal microscopy

Experimental grouping and ultrasonic treatment steps were followed according to 2.3.3, adding 1 ml of PBS to mix the bacteria, then taking 200ul of mixed solution and adding it into a culture medium that liquid culture medium was diluted 1:1 with normal saline, culturing in a 37 °C, 5 % carbon dioxide incubator for 72 h to complete the biofilm construction. The liquid culture medium under the biofilm was absorbed, and the culture dish was dried using a baking plate (DK45, Changzhou Paisijie Medical Equipment Co., Ltd.) to fix the biofilm at the bottom of the culture dish. Then, the biofilm was stained with fluorescein isothiocyanate-labeled concanavalin A (FITC-Con A, Shanghai Maokang Biotechnology Co., Ltd., stored at 2–8 °C). After staining, the growth of Escherichia coli biofilm was observed using a laser confocal microscope, and the biofilm appeared green. In the statistics of Escherichia coli biofilm, the same method as above was used, with the difference being that the green fluorescence intensity was counted and the average and standard deviation of the fluorescence intensity were calculated. The weaker the fluorescence intensity, the less bacterial biofilm there was.

Fig. 1(b) shows the experimental process of this study.

3. Results

3.1. Cavitation-enhanced ROS production

Fig. 2 shows the change in cavitation dose of different concentrations of HMME solution with the intensity of ultrasound, where (a) is 10ug/ml, (b) is 30ug/ml, and (c) is 50ug/ml. The black line in the figure represents the cavitation intensity of physiological saline under the action of ultrasound, which serves as the control group for the experiment. The red line represents the cavitation intensity of the solution with the action of ultrasound without adding MBs. The blue line represents the cavitation intensity of the solution with the action of ultrasound after adding MBs. With the increase in ultrasound intensity, the cavitation intensity after adding MBs had increased significantly. When the ultrasound intensity was 0.15w/cm^2, microbubbles began to play a role. 0.15w/cm^2 was the threshold intensity for microbubbles, and the estimated peak negative pressure (PNP) at this intensity was approximately 0.07 MPa. Noted that the PNP was estimated based on linear acoustics without considering the nonlinear effect and standing waves. When the ultrasound intensity reaches 1.25w/cm^2, the added MBs were completely exhausted, and the cavitation intensity of HMME solutions with concentrations of 10ug/ml and 50ug/ml returned to the same level as that of solutions with the same concentration without adding MBs. The cavitation intensity of HMME solution with a concentration of

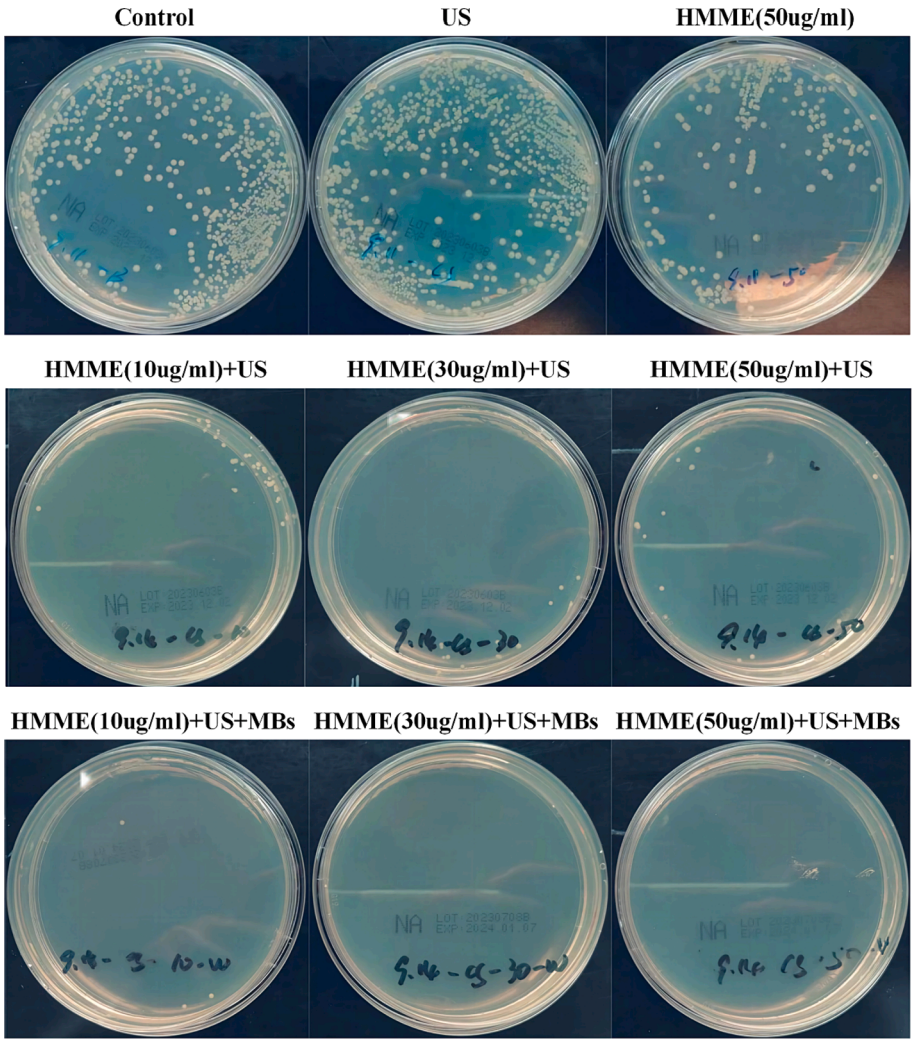

Fig. 4. The growth of bacteria under different conditions in agar solid media for 12 h. (a) Inhibition of Escherichia coli with ultrasound only and with HMME at 50ug/ml only compared to the control group; (b) The inhibitory effect of SDT on Escherichia coli at various concentrations of HMME; (c) The inhibitory effect of SDT with MBs on Escherichia coli at various concentrations of HMME.

30ug/ml decreased compared to that of solutions with the same concentration without adding MBs.

Fig. 3 shows the changes in optical density with time for different concentrations of HMME without/with MBs. The black line represents the optical density curve without ultrasonic treatment; the red line represents the optical density curve after one minute of ultrasonic treatment; the blue line represents the optical density curve after three minutes of ultrasonic treatment; the green line represents the optical density curve after five minutes of ultrasonic treatment; and the purple line represents the optical density curve for different concentrations of HMME. The study found that as the reaction time increased, the optical densities showed a gradual decline trend. During the one-minute reaction time, the optical densities of the three concentrations of sonosensitizers (10ug/ml, 30ug/ml, and 50ug/ml) decreased by 6 %, 10 %, and 10 % due to ultrasonic action, respectively. As the reaction progressed, the solution's absorption peak shifted to the blue, which is because DPBF was gradually consumed during the reaction process (Fig. 3 (a), (b), and (c)).

When MBs were added, it was observed that the absorbance of DPBF decreased significantly at a reaction time of 1 min. The absorbance decrease caused by sonicating with 10ug/ml and 30ug/ml HMME was 69 % and 29 %, respectively. However, when using a HMME concentration of 50ug/ml, the absorbance decrease was only 8 %, indicating that most of the indicators had already been consumed. After ultrasonic treatment for 3 min and 5 min, DPBF was almost completely depleted, and the absorption peak overlapped with that of HMME (Fig. 3(d), (e), and (f)).

As shown in Fig. 3(d), (e), and (f), after adding MBs, the ROS production increased significantly due to the increase in cavitation intensity, In Fig. 3(f), the absorbance decrease caused by a HMME concentration of 50ug/ml was similar to that in Fig. 3(c). This is due to the significant influence of high concentrations of HMME on absorbance detection. However, from the consumption of indicators at different reaction times, it can be seen that the consumption of indicators increased significantly after adding MBs, indicating the generation of more ROS.

3.2. *Inhibition of Escherichia coli activity by sonodynamic therapy*

In this study, the enhanced inhibition of Escherichia coli by using the MBs addition to increase cavitation intensity and ROS production. Fig. 4 shows the growth of bacteria in different conditions in agar culture media under ultrasonic treatment for 12 h, where (a) shows the inhibition of Escherichia coli by without ultrasonic treatment and HMME, with only ultrasound, and with only 50ug/ml HMME; (b) shows the inhibition on Escherichia coli of SDT at different concentrations of HMME; (c) shows the shows the inhibition on Escherichia coli of SDT with MBs at different concentrations of HMME. As shown in Fig. 4 (a),

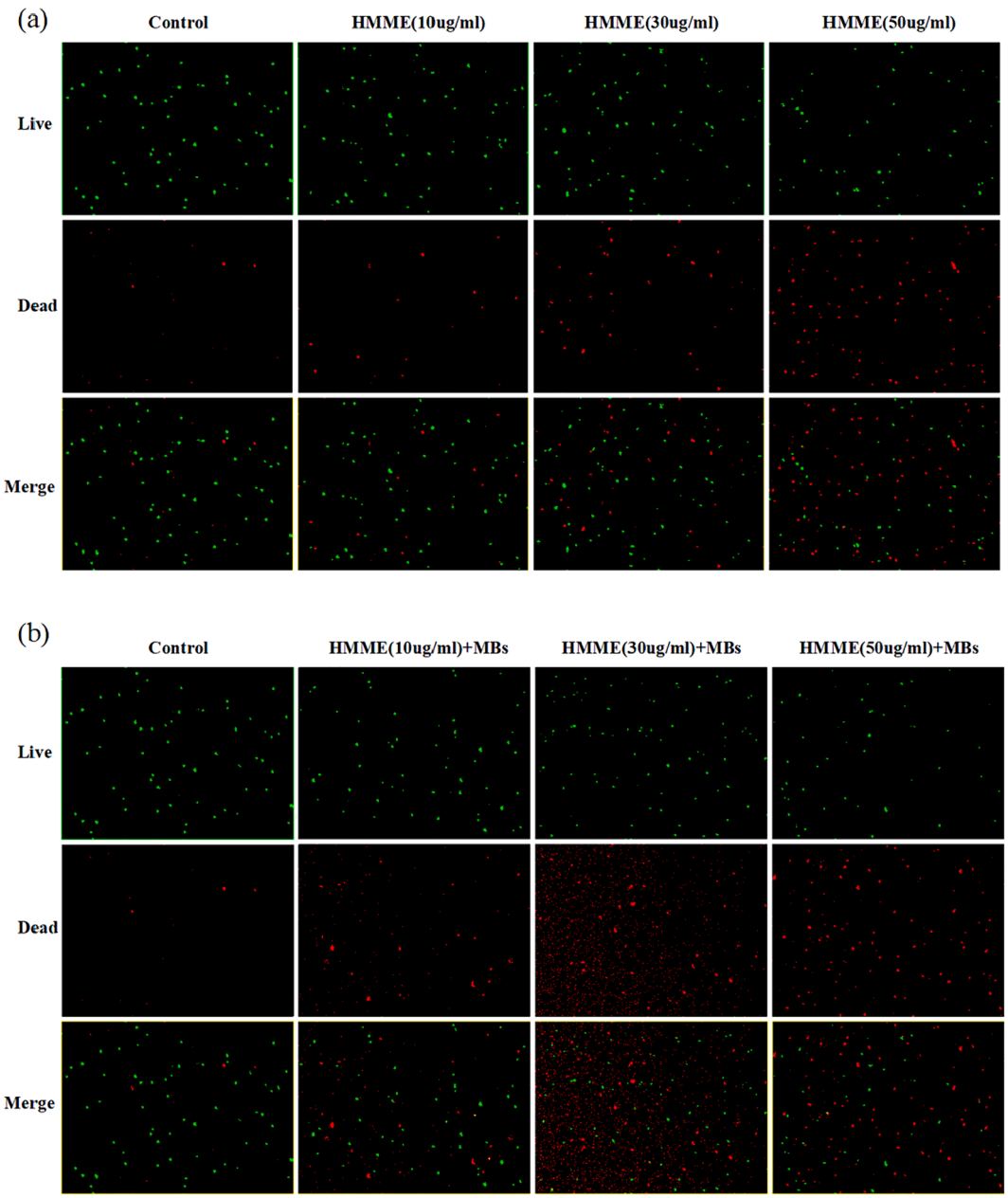

Fig. 5. The death and survival of Escherichia coli cells after being stained with fluorescent dye using a laser confocal microscope, where green represents living cells and red represents dead cells. (a) without MBs, (b) with MBs. (For interpretation of the references to colour in this figure legend, the reader is referred to the web version of this article.)

compared with the control group, neither ultrasonic treatment alone nor HMME alone did not show significant antibacterial effects. This result indicates that the acoustic radiation force (ARF) effect had almost no inhibitory effect on Escherichia coli. As shown in Fig. 4 (b), the result of SDT with various HMME concentration demonstrated the enhanced antibacterial effect. Fig. 4 (c) is the antibacterial result of SDT with MBs. It was seen that after adding MBs, with the increase of the concentration of HMME, the inhibition effect further rose.

Then, we observed the death and survival of Escherichia coli after fluorescence staining using a laser confocal microscope. Fig. 5 (a) shows the dead and living Escherichia coli without MBs, where green represents living cells and red represents dead cells. Compared with the control group, as the concentration of HMME increases, the number of living bacteria (shown as green) gradually decreased, while the number of dead bacteria (shown as red) gradually increased. Fig. 5(b) shows the survival of Escherichia coli when MBs were added, it can be found that the number of dead Escherichia coli at various concentrations of HMME had increased compared to Fig. 5(a).

Fig. 6 gives a statistical analysis of the number of Escherichia coli death and survival in Fig. 5. Compared to the control group, without MBs, the number of dead bacteria increased by 54.2 %, 60 %, and 69.6 % corresponding to HMME concentrations of 10ug/ml, 30 ug/ml, and 50 ug/ml; while after adding MBs, the number of dead bacteria increased by 61.7 %, 71.6 %, and 76.2 % corresponding to HMME concentrations of 10ug/ml, 30 ug/ml, and 50 ug/ml. It is obvious that MBs induced cavitation enhanced the inhibition of Escherichia coli.

Furthermore, we observed the morphological changes in Escherichia coli through scanning electron microscopy (SEM). Fig. 7 shows the morphology of Escherichia coli, where (a) is the control group, (b) is the SDT group, and (c) is SDT with MBs at a HMME concentration of 30ug/ml. Compared to the control group, SDT caused some slight depressions on the surface of bacteria, while after adding MBs, obvious gaps on the

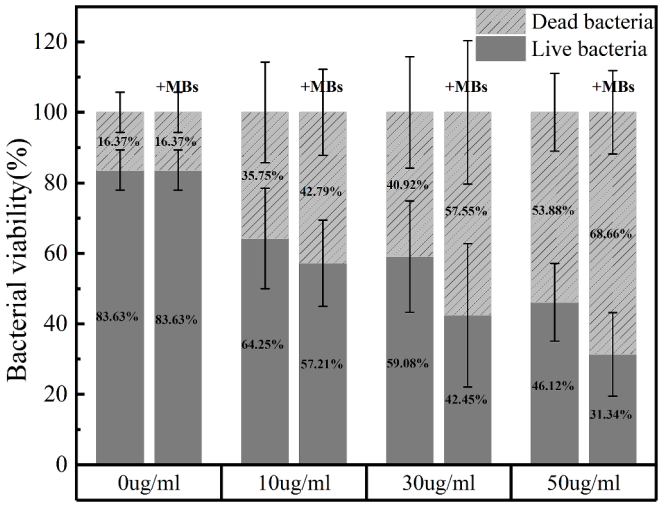

Fig. 6. A quantitative statistical analysis of the number of dead and living bacteria for Fig. 5.

surface of Escherichia coli were observed.

3.3. Inhibition of Escherichia coli biofilm

After Escherichia coli was cultured in liquid medium for 72 h, SDT or SDT with MBs were performed, and the growth of Escherichia coli biofilm was detected by laser confocal microscopy. Fig. 8 shows electron microscope photos of Escherichia coli biofilm, where the upper part shows the inhibition of Escherichia coli biofilm by SDT at different concentrations of HMME, and the lower part shows the inhibition of Escherichia coli biofilm by SDT with MBs at different concentrations of HMME. Compared with the control group, the growth of Escherichia coli biofilm in the experimental group became less and less with the increase of HMME concentration, and the fluorescence intensity became weaker. After adding MBs, the growth of Escherichia coli biofilm in the experimental group further decreased, and the fluorescence intensity further weakened.

Fig. 9 shows the statistical results of fluorescence intensity. Results indicated that compared with the control group, biofilm fluorescence intensity using SDT decreased by 11 %, 32.8 % and 84.1 % corresponding to HMME concentrations of 10ug/ml, 30 ug/ml, and 50 ug/ml; the fluorescence intensity using SDT with MBs decreased by 27.1 %, 80.3 % and 98.2 % corresponding to HMME concentrations of 10ug/ml, 30 ug/ml, and 50 ug/ml.

4. Discussions

In the experiment of detecting ROS production, a set of appropriate ultrasonic parameters is required to be selected. As shown in Fig. 2(b), when MBs were not added, the maximum cavitation intensity was achieved at an ultrasonic intensity of 1.5w/cm^2. In subsequent experiments, in order to achieve the best cavitation effect, the ultrasonic intensity was chosen as 1.5w/cm^2, with an estimated PNP of 0.22 MPa.

As the concentration of HMME increased from 10ug/ml to 30ug/ml, the ultrasonic cavitation threshold showed a significant decreasing

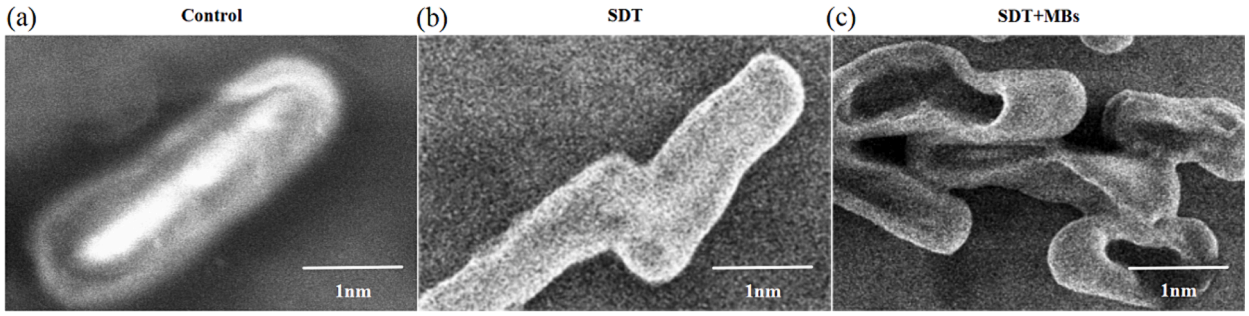

Fig. 7. Morphological structure of Escherichia coli observed using an electron scanning microscope. (a) control group, (b) SDT group, (c) SDT with MBs group.

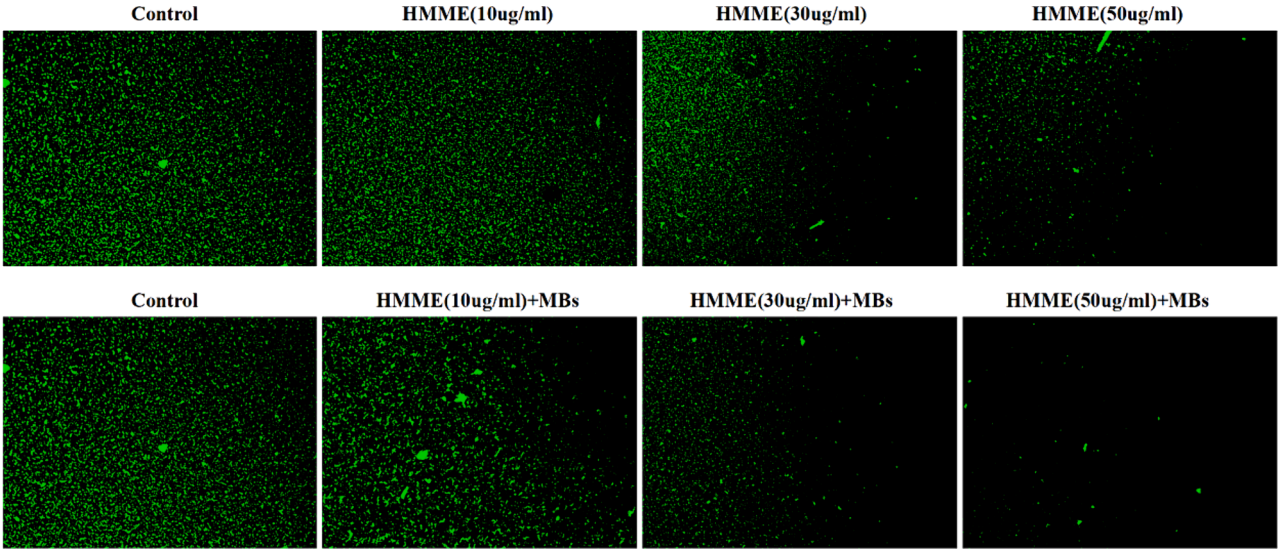

Fig. 8. The inhibitory effect on Escherichia coli biofilm using SDT and SDT with MBs at different concentrations of HMME.

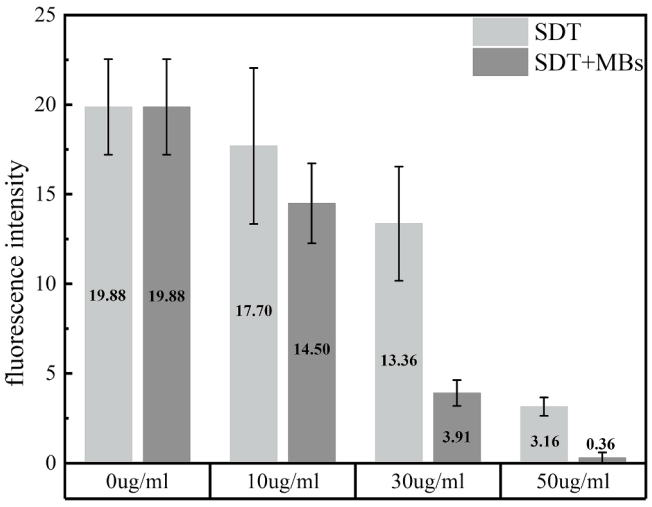

Fig. 9. The statistical analysis of the fluorescence intensity of Escherichia coli biofilm under the synergistic effect of different concentrations of HMME and ultrasound.

trend, as shown in Fig. 2. This phenomenon indicated that an increase in the concentration of sonosensitizers had a positive effect on promoting cavitation reactions. However, when the concentration of HMME further increased from 30ug/ml to 50ug/ml, the cavitation effect no longer occurred. When microbubbles were introduced, both 10ug/ml and 50ug/ml solutions of HMME exhibited cavitation effects before the depletion of microbubbles. However, once the microbubbles were depleted, the cavitation effect also disappeared. This result further confirmed the significant impact of sonosensitizer concentration on the cavitation effect of the solution. This phenomenon is due to the gradual increase in solution viscosity during the elevation of sonosensitizer concentration, and excessively high solution viscosity inhibits the cavitation effect.

Under the condition of not adding microbubbles, no cavitation effect was observed in the 10ug/ml and 50ug/ml HMME solutions shown in Fig. 2. However, in the reactive oxygen species (ROS) generation test shown in Fig. 3, both the 10ug/ml and 50ug/ml HMME solutions produced ROS with increased ultrasonic treatment time. When microbubbles were introduced, the ROS production of different concentrations of sonosensitizers in Fig. 3 further increased with the extension of ultrasonic treatment time, indicating that the addition of microbubbles has a significant promoting effect on ROS generation. Comprehensive analysis of the results from the cavitation dose experiment and the ROS generation test shows that in the process of SDT, cavitation effect does not determine the generation of ROS, but can only increase its yield.

This study suggests that during the process of SDT, cavitation effects play a dual role. On one hand, it can enhance the production of reactive oxygen species under ultrasonic conditions. On the other hand, mechanical actions such as microjets, shock waves, and shear forces generated by cavitation effects can damage the cell walls of microorganisms and other structures, thereby making it easier for reactive oxygen species to kill microbes. In subsequent experiments, changes in the morphology and structure of bacteria after ultrasonic treatment were observed through scanning electron microscopy, verifying the viewpoint that microbial cell walls are destroyed.

In the study of antibacterial effects of SDT, Zhuang[21] and Zhang [26] used HMME as a sonosensitizer to inhibit Porphyromonas gingivalis and Staphylococcus aureus. In their study, the concentrations of HMME used were 50ug/ml and 40ug/ml respectively; no MBs were added and relative high ultrasound intensities were used (6w/cm^2 [21] and 3w/cm^2 [26]). Although the results of SDT exhibited good antibacterial ability, the relative high intensity ultrasound posed a significant safety risk. In this study, we reduced the required ultrasound intensity by adding MBs, achieving good antibacterial effects with only 1.5w/cm^2 of ultrasound intensity. Based on the experimental results of cavitation dose experiments and ROS detection experiments, optimized acoustic intensity and spatiotemporal control of microbubble-mediated cavitation are crucial to biosafety of the SDT application.

Through the experimental verification of laser confocal microscopy and agar culture medium antibacterial experiments, Microbubble-mediated cavitation can produce more ROS, and further improved the inhibitory ability of SDT on Escherichia coli. For example, after adding MBs, the number of dead bacteria increased by 28.9 % under the condition of a HMME concentration of 30ug/ml, indicating that there was a good improvement effect on the antibacterial ability of SDT. The results demonstrated that with the addition of MBs and the increase in the concentration of HMME, the inhibition effect on Escherichia coli was gradually improving.

To explain why the combination of HMME and MBs can inhibit bacteria, this study observed the morphology and structure of Escherichia coli through SEM, as shown in Fig. 7. The results indicate that the enhancement of cavitation intensity brought by MBs not only promoted the generation of ROS, but also intensified the changes in bacterial surface structure. The cell walls of bacteria were damaged by the cavitation effect, which led to a large amount of ROS being able to penetrate the cell wall and caused more direct damage to the cell membrane and internal structures of bacteria.

5. Conclusions

In this article, through a series of studies such as the detection of cavitation intensity and absorbance, experiments on anti-Escherichia coli and inhibition of Escherichia coli biofilm, as well as observations on the morphological structure of Escherichia coli, it is concluded that Microbubble-mediated cavitation can promote the inhibitory effect of SDT on bacteria and biofilms, which mainly comes from two aspects. Firstly, the addition of MBs can significantly increase the cavitation intensity, resulting in more active oxygen production. Secondly, the enhanced cavitation effect brought by MBs can more obviously change the surface morphology of bacteria, making it easier for active oxygen to penetrate through the cell wall and cause damage to bacteria.

It should be pointed out that, in the process of PCD waveform collection, due to limitations in the storage depth and data transmission time of the digital oscilloscope, and considering the balance among multiple experimental factors, a sampling frequency of 20 MHz was adopted, with a sampling data point of 8192 and a corresponding waveform acquisition time of about 200 microseconds. The acquisition time of individual PCD waveforms was slightly shorter compared to the excitation time of the ultrasonic pulse. However, since a larger pulse width and duty cycle were adopted for the ultrasound excitation pulse, relatively high concentrations of microbubbles and sonosensitizers were also applied in the experiments to ensure that cavitation activity could reach relatively stable state during the whole ultrasonic excitation process. Therefore, 8192 data points captured within a time duration of 200 microseconds should be sufficient for accurate FFT analysis, and could provide enough data support to quantitatively compare the cavitation intensity levels generated under different conditions at a certain extent. Of course, in future studies, we will further improve the experimental design to perform sufficiently long-term data collection of PCD waveforms, so that more accurate quantification of cavitation dose could be achieved.

CRediT authorship contribution statement

Changlong Li: Validation, Software, Methodology, Investigation. **Fengmeng Teng:** Validation, Software, Methodology, Investigation. **Fengmin Wu:** Writing – review & editing, Writing – original draft, Validation, Supervision, Methodology, Investigation,

Conceptualization. **Hui Zhang:** Validation, Methodology, Investigation. **Chunbing Zhang:** Writing – original draft, Validation, Supervision, Methodology, Investigation, Conceptualization. **Dong Zhang:** Writing – review & editing, Writing – original draft, Supervision, Methodology, Investigation, Funding acquisition, Conceptualization.

Declaration of competing interest

The authors declare that they have no known competing financial interests or personal relationships that could have appeared to influence the work reported in this paper.

Acknowledgments

This work was supported by the National Key R&D Program of China (2022YFB3204303), the National Natural Science Foundation of China (No. 11934009), the Fundamental Research Funds for the Central Universities (No. 020414380195), and the Foundation of State Key Laboratory of Ultrasound in Medicine and Engineering (Grant No. 2022KFKT021).

References

[1] K.E. Pristov, M.A. Ghannoum, Resistance of Candida to azoles and echinocandins worldwide, Clin. Microbiol. Infect. 25 (7) (2019) 792–798.
[2] J.R. Mediavilla, A. Patrawalla, L. Chen, et al., Colistin- and Carbapenem-resistant Escherichia coli Harboring mcr-1 and blaNDM-5, causing a complicated Urinary Tract infection in a patient from the United States, Microbial Biol. 7 (4) (2016) e01191–e01216.
[3] L.M.Q. Alareqi, M.A.K. Mahdy, Y.L. Lau, et al., Molecular markers associated with resistance to commonly used antimalarial drugs among Plasmodium falciparum isolates from a malaria-endemic area in taiz governorate-Yemen during the transmission season, Acta Trop. 162 (2016) 174–179.
[4] S.H. Podolsky, The evolving response to antibiotic resistance (1945–2018), Palgrave Commun 4 (124) (2018) 1–8.
[5] C.L. Jia, G.S. Jiang, C.H. Li, et al., Effect of dental plaque control on infection of Helicobacter pylori in gastric mucosa, J. Periodontol. 80 (10) (2009) 1606–1609.
[6] Y. Sun, D. Xing, L. Shen, et al., Bactericidal effects of hematoporphyrin monomethyl ether-mediated photosensitization against pathogenic communities from supragingival plaque, Appl. Microbiol. Biotechnol. 97 (2013) 5079–5087.
[7] J. O'Neill, Tackling drug-resistant infections globally: final report and recommendations, Review on Antimicrobial Resistance, London, 2016.
[8] M.H. Muhammad, A.L. Idris, X. Fan, et al., Beyond risk: bacterial biofilms and their regulating approaches, Front. Microbiol. 11 (2020) 928.
[9] S.P. Songca, Y. Adjei, Applications of antimicrobial photodynamic therapy against bacterial biofilms, Int. J. Mol. Sci. 23 (6) (2022) 3209.
[10] Y. Xu, S. Liu, H. Zhao, et al., Ultrasonic irradiation enhanced the efficacy of antimicrobial photodynamic therapy against methicillin-resistant Staphylococcus aureus biofilm, Ultrason. Sonochem. 97 (2023) 106423.
[11] M. Wainwright, Photodynamic antimicrobial chemotherapy (PACT), J. Antimicrob. Chemother. 42 (1) (1998) 13–28.
[12] Agostinis P, Berg K, Cengel K A, et al. Photodynamic therapy of cancer: an update. CA: Cancer J. Clin., 2011, 61(4): 250-281.
[13] D. Van Straten, V. Mashayekhi, H.S. De Bruijn, et al., Oncologic photodynamic therapy: basic principles, current clinical status and future directions, Cancers 9 (2) (2017) 19.
[14] C.P. Sabino, M. Wainwright, M.S. Ribeiro, et al., Global priority multidrug-resistant pathogens do not resist photodynamic therapy, J. Photochem. Photobiol. B Biol. 208 (2020) 111893.
[15] M. Antunes, W.C. de Melo, R. Celiešiūtė-Germanienė, P. Šimonis, et al., Antimicrobial photodynamic therapy (aPDT) for biofilm treatments. possible synergy between aPDT and pulsed electric fields, Virulence 12 (1) (2021) 2247–2272.
[16] J. Kim, Y. Jo, K. Na, Photodynamic therapy with smart nanomedicine, Arch. Pharm. Res. 43 (2020) 22–31.
[17] M.J. Page, J.E. McKenzie, P.M. Bossuyt, et al., The PRISMA 2020 statement: an updated guideline for reporting systematic reviews, Int. J. Surg. 88 (2021) 105906.
[18] Q. Xu, W. Xiu, Q. Li, et al., Emerging nanosonosensitizers augment sonodynamic-mediated antimicrobial therapies, Materials Today Bio (2023) 100559.
[19] P.Y. Xu, R.K. Kankala, S.B. Wang, et al., Sonodynamic therapy-based nanoplatforms for combating bacterial infections, Ultrason. Sonochem. 106617 (2023).
[20] R. Wang, Q. Liu, A. Gao, et al., Recent developments of sonodynamic therapy in antibacterial application, Nanoscale 14 (36) (2022) 12999–13017.
[21] D. Zhuang, C. Hou, L. Bi, et al., Sonodynamic effects of hematoporphyrin monomethyl ether on Staphylococcus aureus in vitro, FEMS Microbioloy Letters 361 (2) (2014) 174–180.
[22] T. Kondo, E. Kano, The possibility of ultrasonic cancer therapy and some of the difficulties implications of the thermal and nonthermal effects, Thermal Medicine (Japan. J. Hypertherm. Oncol.) 6 (1) (1990) 1–18.
[23] A.P. McHale, J.F. Callan, N. Nomikou, et al., Sonodynamic therapy: concept, mechanism and application to cancer treatment, Therapeutic Ultrasound (2016) 429–450.
[24] T. Kondo, S.I. Umemura, K. Tanabe, et al., Novel therapeutic applications of ultrasound. utilization of thermal and cavitational effects, Thermal Medicine (Japan J. Hypertherm. Oncol.) 16 (4) (2000) 203–216.
[25] L.B. Feril, T. Kondo, S. Umemura, et al., Sound waves and antineoplastic drugs: the possibility of an enhanced combined anticancer therapy, J. Med. Ultrason. 29 (2002) 173–187.
[26] Y. Zhang, H. Zhang, D. Zhuang, et al., Hematoporphyrin monomethyl ether mediated sonodynamic antimicrobial chemotherapy on porphyromonas gingivalis in vitro, Microb. Pathog. 144 (2020) 104192.
[27] X. Wang, M. Ip, A.W. Leung, et al., Sonodynamic action of curcumin on foodborne bacteria Bacillus cereus and Escherichia coli, Ultrasonics 62 (2015) 75–79.
[28] M.L. Bhavya, H.U. Hebbar, Sono-photodynamic inactivation of Escherichia coli and Staphylococcus aureus in orange juice, Ultrason. Sonochem. 57 (2019) 108–115.
[29] C. Xu, J. Dong, M. Ip, et al., Sonodynamic action of chlorin e6 on Staphylococcus aureus and Escherichia coli, Ultrasonics 64 (2016) 54–57.
[30] M. Yang, S. Xie, V.P. Adhikari, et al., The synergistic fungicidal effect of low-frequency and low-intensity ultrasound with amphotericin B-loaded nanoparticles on C. albicans in vitro, Int. J. Pharm. 542 (1–2) (2018) 232–241.
[31] Y. Wang, Y. Sun, S. Liu, et al., Preparation of sonoactivated TiO2-DVDMS nanocomposite for enhanced antibacterial activity, Ultrason. Sonochem. 63 (2020) 104968.
[32] D. Wang, F. Zhou, D. Lai, et al., Curcumin-mediated sono/photodynamic treatment preserved the quality of shrimp surimi and influenced its microbial community changes during refrigerated storage, Ultrason. Sonochem. 78 (2021) 105715.
[33] K. Kooiman, S. Roovers, S.A.G. Langeveld, et al., Ultrasound-responsive cavitation nuclei for therapy and drug delivery, Ultrasound Med. Biol. 46 (6) (2020) 1296–1325.
[34] B.D. Lindsey, J.D. Rojas, P.A. Dayton, On the relationship between microbubble fragmentation, deflation and broadband superharmonic signal production, Ultrasound Med. Biol. 41 (6) (2015) 1711–1725.
[35] J. Kim, K.J.B. Bautista, R.M. Deruiter, et al., An analysis of sonothrombolysis and cavitation for retracted and unretracted clots using microbubbles versus low-boiling-point nanodroplets, IEEE Trans. Ultrason. Ferroelectr. Freq. Control 69 (2) (2021) 711–719.
[36] K. Bilmin, T. Kujawska, W. Secomski, et al., 5-aminolevulinic acid-mediated sonosensitization of rat RG2 glioma cells in vitro, Folia Neuropathol. 54 (3) (2016) 234–240.
[37] H. Chen, X. Zhou, Y. Gao, et al., Recent progress in development of new sonosensitizers for sonodynamic cancer therapy, Drug Discov. Today 19 (4) (2014) 502–509.
[38] M.M. Rahman, K. Ninomiya, C. Ogino, et al., Ultrasound-induced membrane lipid peroxidation and cell damage of Escherichia coli in the presence of non-woven TiO2 fabrics, Ultrason. Sonochem. 17 (4) (2010) 738–743.
[39] E. Li, Y. Sun, G. Lv, et al., Sinoporphyrin sodium based sonodynamic therapy induces anti-tumor effects in hepatocellular carcinoma and activates p53/caspase 3 axis, Int. J. Biochem. Cell Biol. 113 (2019) 104–114.
[40] K.B. Bader, K.J. Haworth, H. Shekhar, et al., Efficacy of histotripsy combined with rt-PA in vitro, Phys. Med. Biol. 61 (14) (2016) 5253.
[41] J. Kim, R.M. DeRuiter, L. Goel, et al., A comparison of sonothrombolysis in aged clots between low-boiling-point phase-change nanodroplets and microbubbles of the same composition, Ultrasound Med. Biol. 46 (11) (2020) 3059–3068.
[42] Y. Gu, C. Chen, J. Tu, et al., Harmonic responses and cavitation activity of encapsulated microbubbles coupled with magnetic nanoparticles, Ultrason. Sonochem. 29 (2016) 309–316.